Annealing of Commercial Block Polypropylene. II. Behavior of Poly(ethylene-*co*-propylene) Component

JUN-ICHI ITO,* KATSUO MITANI, and YUKIO MIZUTANI

Fujisawa Laboratory, Tokuyama Soda Co., Ltd., 2051 Endo, Fujisawa City, Kanagawa 252, Japan

SYNOPSIS

Moldings of ethylene–propylene block copolymer (block PP) are improved by annealing in their tensile impact strength (TIS) and brittle temperature (Tb). To elucidate the mechanism, the role of the poly(ethylene-*co*-propylene) (PEP) component was studied, and the component extracted with *n*-heptane from annealed test pieces was subjected to characterization by a fractionation technique. It is found that recrystallization takes place by annealing in the PP matrix and results in segregation of atactic PP and high molecular weight amorphous PEP from the crystal region to the amorphous region. Furthermore, crystalline PEP also undergoes recrystallization by annealing, increasing the miscibility in the interface of PP and PEP. These phenomena in the solid phase are discussed in connection with the annealing effect related to impact strength. © 1992 John Wiley & Sons, Inc.

INTRODUCTION

Generally, so-called block polypropylene (block PP) is prepared by copolymerizing propylene with ethylene at the later stage of polymerization to improve impact strength. Block PP consists of the three components: PP, polyethylene (PE), and poly(ethylene-*co*-propylene) (PEP), and a small domain having the shape of a PE particle covered with PEP is dispersed in the PP matrix.[1-5] In the preceding paper,[6] we reported the effect of annealing on the mechanical properties of block PP whereby that annealing of a molding near its melting point could remarkably increase its impact strength. This annealing effect is contradictory to the general expectation that annealing of a molding of block PP, a crystalline polymer, would increase its crystallinity and, hence, its brittleness.

We consider the reason why annealing of moldings increases tensile impact strength (TIS) and brittle temperature (Tb) to be as follows: First, the morphological change is engendered due to annealing: The amorphous component is rejected from the disturbed crystal region to the undisturbed amorphous region as a result of the recrystallization of the PP matrix phase and it causes a decrease of the glass transition temperature (T_g) of the material as a whole.[7,8] Second, annealing probably engenders an interdiffusion at the interface between the dispersed phase of the PEP and PP matrix to effect an increase in the bonding strength of the interface.

The behavior of the PEP component was studied as a means for verifying the mechanism described above. Therefore, the authors investigated the difference of components in the *n*-heptane-extracted polymer (amorphous polymers chiefly consisting of atactic PP and PEP) by using annealed and unannealed polymers, which makes it possible to consider the change inside the solid phase. Accordingly, the *n*-heptane-extracted polymers were characterized in detail by fractionation so as to be able to discuss the evident annealing effect of block PP.

EXPERIMENTAL

The block PP used was a product of Tokuyama Soda Co. (block PP-A), whose properties are listed in Table I. The preparation (compression molding) of test pieces for the measurements were performed in the same manner as in previous studies.[9] Annealing was carried out as follows: Test pieces wrapped in

* To whom correspondence should be addressed.

Journal of Applied Polymer Science, Vol. 46, 1235–1243 (1992)
 CCC 0021-8995/92/071235-09

aluminum foil were placed in a glass vessel; the vessel was evacuated and heated for 3 h in an air-oven controlled at 140°C; then, the actual temperature was checked by a thermometer placed beside the vessel. Samples for fractionation were prepared as follows: Unannealed or annealed TIS test pieces were powdered with dry ice by using a coffee mill until it passed through a 40-mesh screen; the powder was subjected to extraction with *n*-heptane in a Soxhlet for 13 h; then, the extracted polymer was precipitated with a large amount of methanol and vacuum-dried to make a sample for fractionation. After the extracting operation, a small amount of 2,6-di-*tert*-butyl-*p*-cresol (BHT) was added to the solvent as an oxidation inhibitor. Hereafter, the polymer extracted from unannealed TIS test pieces will be called A-1, and the one from annealed TIS test pieces, A-2.

The column fractionation of the *n*-heptane-extracted polymers was conducted according to the well-known Desreux method,[10] by which fractionation is carried out corresponding to molecular weight, chemical composition, or monomer sequence length. This is the gradient elution method, in which a polymer is thinly coated on the surface of an inorganic support and extracted at a constant temperature by elution liquids with various mixing ratios of solvent and nonsolvent. The column used was made of glass and of a reflux type with a boiler (capacity: 2 L), which was used by Hall.[11] For the method of operation and selection of solvents, nonsolvents, and others, according to the methods of Saijo et al.[12] and Ogawa et al.,[13] kerosene as solvent, butyl carbitol as nonsolvent, celite as the support, and cyclohexanol as heating medium were used. The amount of polymer loaded in each fractionation was 10 g.

Characterization of the fractionated samples was made in the same manner as in the previous report,[9] using the differential scanning calorimeter (DSC), ^{13}C-NMR, and gel permeation chromatography (GPC). The fractionated polymers or polymer fractions obtained by use of elution liquids with kerosene concentration of more than 45% were too small in quantity to be characterized. Preceding the measurement of the heat of fusion, the samples for DSC measurement were subjected to melting in the DSC sample holder at 230°C for 15 min, kept at 140°C for 3 h, and kept further at 110°C for 3 h, and then allowed to cool to room temperature. The measurement of heat of fusion was made with a heating rate of 10°C/min.

RESULTS AND DISCUSSION

Mechanical Properties of Annealed Block PP-A

Table I shows that annealing of block PP-A, like the annealing effect with a PP/PEP blend, increases its TIS, Tb, yield strength (YS), elastic modulus (E), and Rockwell hardness (H_R) with an increase in crystallinity and decreases its tensile strength (TS) and elongation (Elong.).

Wondering whether annealing would affect the size of spherulites, the middle of the section of a TIS test piece used in Table I was examined with a polarization microscope to find that the average size of the spherulites is constant at 80 microns regardless of being annealed or unannealed. The increase in crystallinity on annealing, therefore, is considered to be the result of a change in the fine texture.

n-Heptane-Extraction of Block PP-A

Previous studies[6,9,14] have revealed that PEP plays a significant role in the effect of annealing on impact strength. It was intended, therefore, to obtain direct information of the annealing effect by analysis of the *n*-heptane extracts consisting of PEP and atactic PP.

When the powdered TIS test pieces were subjected to extraction with *n*-heptane in a Soxhlet,

Table I Mechanical Properties of Annealed Commercial Block PP-A[a]

Annealing Condition	TIS (kg cm/cm^2)	Tb (°C)	YS (kg/cm^2)	TS (kg/cm^2)	$E \times 10^{-3}$ (kg/cm^2)	Elong. (%)	H_R	χc[b] (%)	Extracted[c] Polymer (wt %)
Unannealed	70	−0.5	238	346	2.7	960	85	56.8	8.0 (A-1)
Annealed (140°C, 3 hr)	121	−9.0	265	310	3.2	820	88	59.7	6.5 (A-2)

[a] Block PP-A: MFI = 6.0 g/10 min; ethylene content = 6.2 wt %; talc content = 0.
[b] The crystallinity (χc) was measured by X-ray diffraction.
[c] Extracted for 13 h by *n*-heptane with Soxhlet-type apparatus.

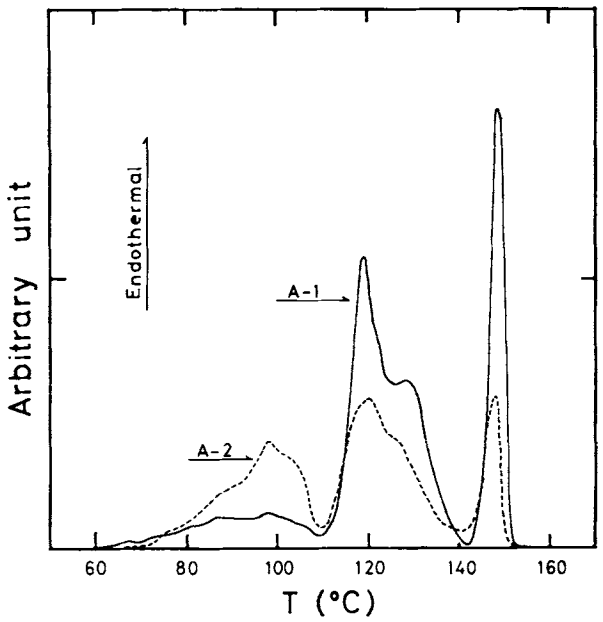

Figure 1 Normalized DSC curves of *n*-heptane extracted polymers (A-1 and A-2). Heating rate = 10°C/min: A-1 (7.2 cal/g); A-2 (3.6 cal/g).

the extraction rates were 6.5 wt % for the unannealed test piece (A-1) and 8.0 wt % for the annealed one (A-2), showing a distinct difference. On the other hand, as for the ethylene contents obtained by ^{13}C-NMR analysis, block PP-A as a whole had an ethylene content of 6.2 wt %, while the ethylene contents in A-1 and A-2 were 3.0 and 1.8 wt % of the whole block PP-A, respectively. The ethylene fraction not extracted with *n*-heptane is elucidated to remain in the PP matrix chiefly as PE dispersion particles and partly as PEP of crystallized or a dispersed form hardly extractable.[6]

Figure 1 shows the DSC curve for the *n*-heptane-extracted polymer. The endothermic peaks at about 120°C and about 150°C represent the fusion curves for PE and PP, respectively. The endothermic peak observed below 110°C probably stands for a partial fusion of crystalline PEP. The enthalpies of fusion for A-1 and A-2 are 7.2 and 3.6 cal/g, respectively. The crystallinity of the *n*-heptane-extract of the annealed molding (A-2) decreased to half, suggesting that annealing results in the change in the composition of the extracted polymer.

Column Fractionation of *n*-Hexane-Extracted Polymer

Figure 2 shows the result of fractionation, that is, the weight of each fraction for various composition of the elution liquid. Here, the value in Figure 2 is reduced to the weight fraction to the whole block PP-A.

In general, with an increase in the kerosene concentration of the elution liquid, the ethylene content of the fractional polymer increased in the direction from PP-rich to PEP-rich and then to PE-rich. Also, a fractionation according to molecular weight, from low molecular to high molecular weight, occurred simultaneously with the fractionation according to chemical composition.

A fractional polymer for an elution liquid of kerosene *n* vol % will be abbreviated as Fn hereafter. The fraction of kerosene 0 vol % (abbreviated as F0) normally consists of low molecular weight PP, but is found to contain low molecular weight PEP in the present fractionation. The fractions beyond F5 are the polymers corresponding to PEP, and especially those beyond F40 were PEP with high ethylene content. As for the weight fractions for A-2, those in the range of F0–F25 are all smaller as compared with A-1 and only F35 was peculiarly larger in contrast. This F35 fraction is considered to be an important key for understanding the annealing effect on the impact strength of block PP.

Table II shows the weight fractions for A-1 and A-2. From those data, *n*-heptane extracts are found to consist chiefly of PEP.

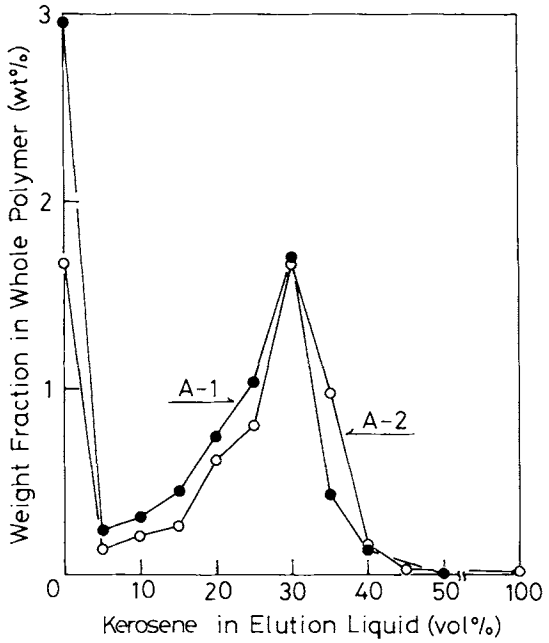

Figure 2 Results of the column fractionations for A-1 and A-2. The weight fractions are normalized to the value to the whole block PP-A.

Table II Weight Fractions for A-1 and A-2 Polymers

	F0	F5–F30	F35	F40+
A-1	2.96	4.48	0.43	0.13
A-2	1.67	3.66	0.97	0.20

The unit is wt %.

Characterization of Fractional Polymers

Fractional polymers were subjected to measurements of ethylene–propylene composition, isotacticity, heat of fusion, molecular weight, and molecular weight distribution by ^{13}C-NMR, DSC, and GPC in order to characterize each component.

Figure 3 shows the molar fraction of ethylene for each fractional polymer determined by ^{13}C-NMR. F0 is found to be a mixture of the principal component PP with PEP. F5–F30 are found to be PEP containing 35–40 mol % of ethylene.

The fraction F35 is understood to be a fractional component corresponding to the boundary conditions under which a random PEP shifts to a polymer with the character of PE. It is found that F35 of A-1 corresponds to an ethylene-rich PEP fractional region, and F35 of A-2 corresponds to the last fraction in the random PEP fractional region. F40 fractions of both A-1 and A-2 are found to consist of PEP with more ethylene.

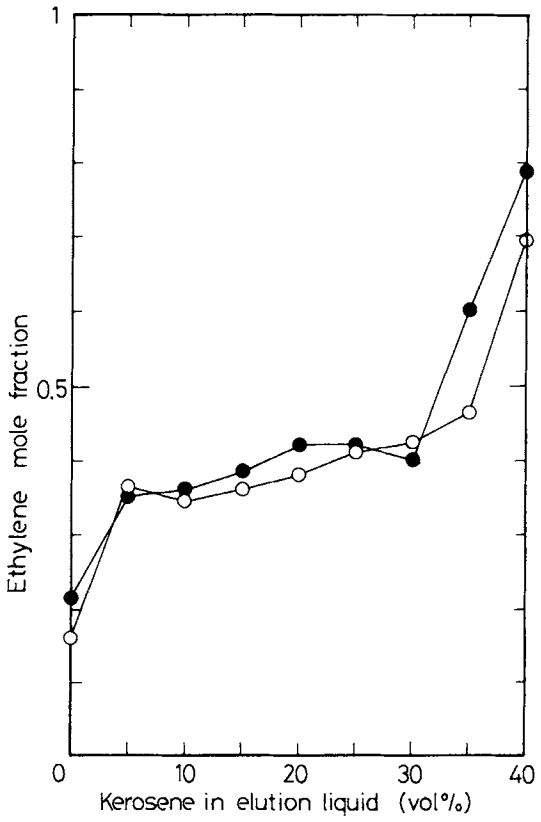

Figure 3 Ethylene content in each fractional polymer determined by ^{13}C-NMR: (●) A-1; (○) A-2.

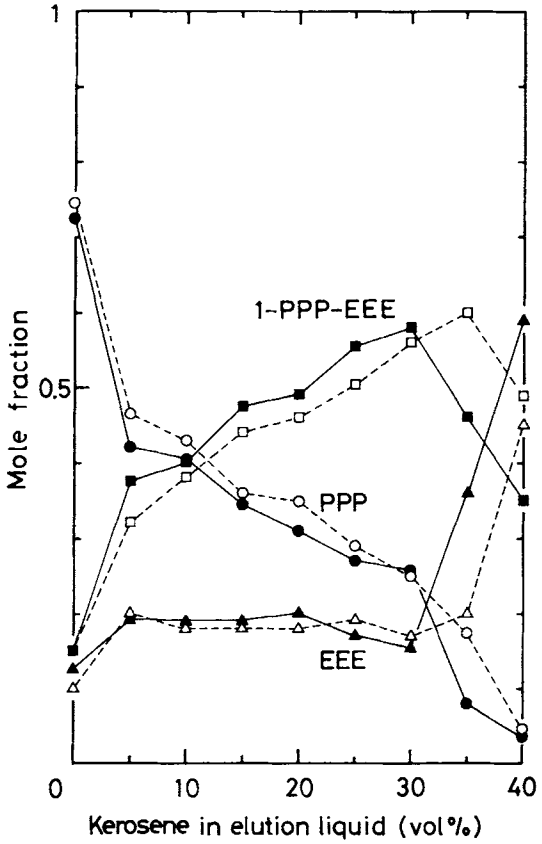

Figure 4 Distribution of the triad sequences in each fractional polymer determined by ^{13}C-NMR: (solid lines) A-1; (dashed lines) A-2.

Figure 4 indicates the rate of the triad sequences in each fraction obtained by ^{13}C-NMR analysis. PPP and EEE express segments consisting of three consecutively linked units of propylene and ethylene, respectively. The value of 1-PPP–EEE has been used as an indication of the randomness of the ethylene–propylene sequence.

The molecular structure of the PEP component of the general block PP produced by the Ziegler–Natta polymerization can be conceived as follows[15]:

$$\text{P}\cdot\cdot\text{P}-\text{E}\cdot\cdot\text{E},\quad \text{P}\cdot\cdot\text{P}-(\text{EP}),$$

$$(\text{EP})-(\text{EP}),\quad \text{P}\cdot\cdot\text{P}-(\text{EP})-\text{P}\cdot\cdot\text{P}$$

and multisegment chains such as

$$P\cdot\cdot P-E\cdot\cdot E-P\cdot\cdot P-E\cdot\cdot E,$$

$$P\cdot\cdot P-(EP)-P\cdot\cdot P-(EP), \text{ or}$$

$$(EP)'-(EP)-(EP)'-(EP)$$

where E · · E, P · · P, and (EP) [or (EP)'] represent long segments of ethylene, propylene, and copolymerized ethylene–propylene, respectively.

In addition, sequences as follows can be presumed as the structure of (EP):

Random: EPPEEPEPPPEPEEPEPPE–

Block: EEPEPPPPPPEPEEEEEEP–

Tapered: PPPPPEPPP–EPPPEPPEE–

PEEEPEEEEE

F0 fractions of A-1 and A-2 contain PP as the chief component, and the value of the 1-PPP—EEE that is about 0.15 indicates the presence of the PEP component in these fractions. The PEP component of F5–F30 is characteristic: The frequency of randomness in 1-PPP—EEE gradually increases with the kerosene concentration of the elution liquid, because the frequency of the PPP sequence gradually decreases and that of the EEE sequence remains constant. The constancy of the frequency of the EEE sequence might be characteristic of the polymerization process of the PEP component. In addition, A-2 has a little longer sequence of propylene and a little less randomness in comparison to A-1 for the PEP component of F5–F30 in general. As to the F35 fraction, A-1 is a PEP having a long ethylene sequence and A-2 corresponds to PEP having the most random molecular structure. F40 fractions of both A-1 and A-2 consist of PEP with a further longer ethylene sequence. The PEP component in general, A-2, or the *n*-heptane-extract from the annealed molding, consists of PEP with a little longer propylene sequence and a little less randomness as compared with A-1 or with the blank extract from the unannealed molding.

Figure 5 is a plotting of triad tacticity for further investigation of the tacticity of the propylene sequence (PPP) as shown in Figure 4. The symbol "mm" denotes an isotactic triad; "mr," a heterotactic; and "rr," a syndiotactic. Data for the fractions beyond F35 were neglected because a sufficient accuracy of measurement could not be attained with them. Isotacticities of the fractions of A-2 were similarly smaller than those of A-1, presumably because

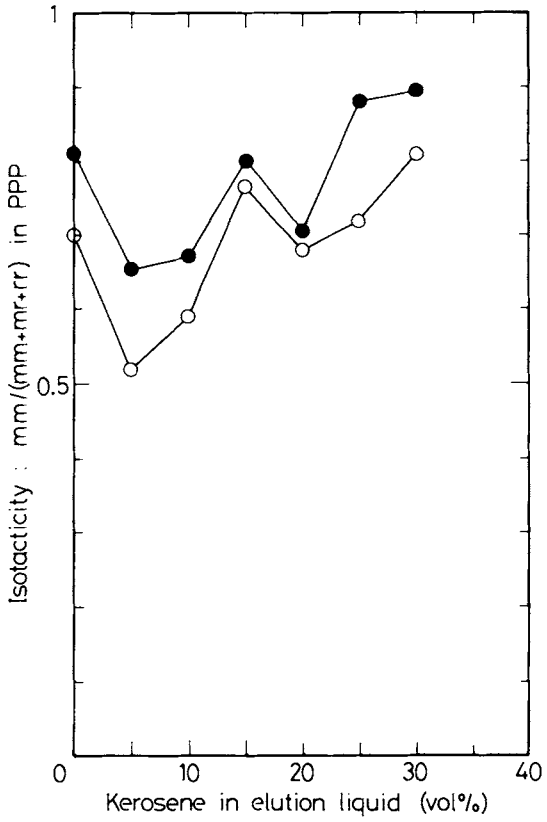

Figure 5 Isotacticity of each fractional polymer determined by ^{13}C-NMR: (●) A-1; (○) A-2.

annealing promoted recrystallization of the highly isotactic propylene sequence so as to make it difficult to extract.

Figure 6 illustrates the results of DSC analysis of fractional polymers. Each DSC curve is normalized in terms of enthalpy of fusion. At the right side of the figure, the enthalpy of fusion for each fraction is plotted. (There was no measurement of F45 of A-1, because its sample was not available.) All fractions of A-2 are found to be lower in crystallinity than those of A-1. The fractions beyond F5, consisting of the PEP component, are found to be very random, especially with A-2. This shows almost undetectable peaks for propylene crystals near 150°C and for ethylene crystals near 120°C. The peak below 110°C indicates the fusion curve for the ethylene–propylene sequence. The results of the DSC measurement also suggest that annealing promotes recrystallization of the crystalline PEP and it makes the crystalline PEP difficult to extract with *n*-heptane. The F35 fraction of A-2 along with F30 are found to be PEP with lower crystallinity.

Figure 7 shows the results of the molecular weight measurement with GPC of fractional polymers. The

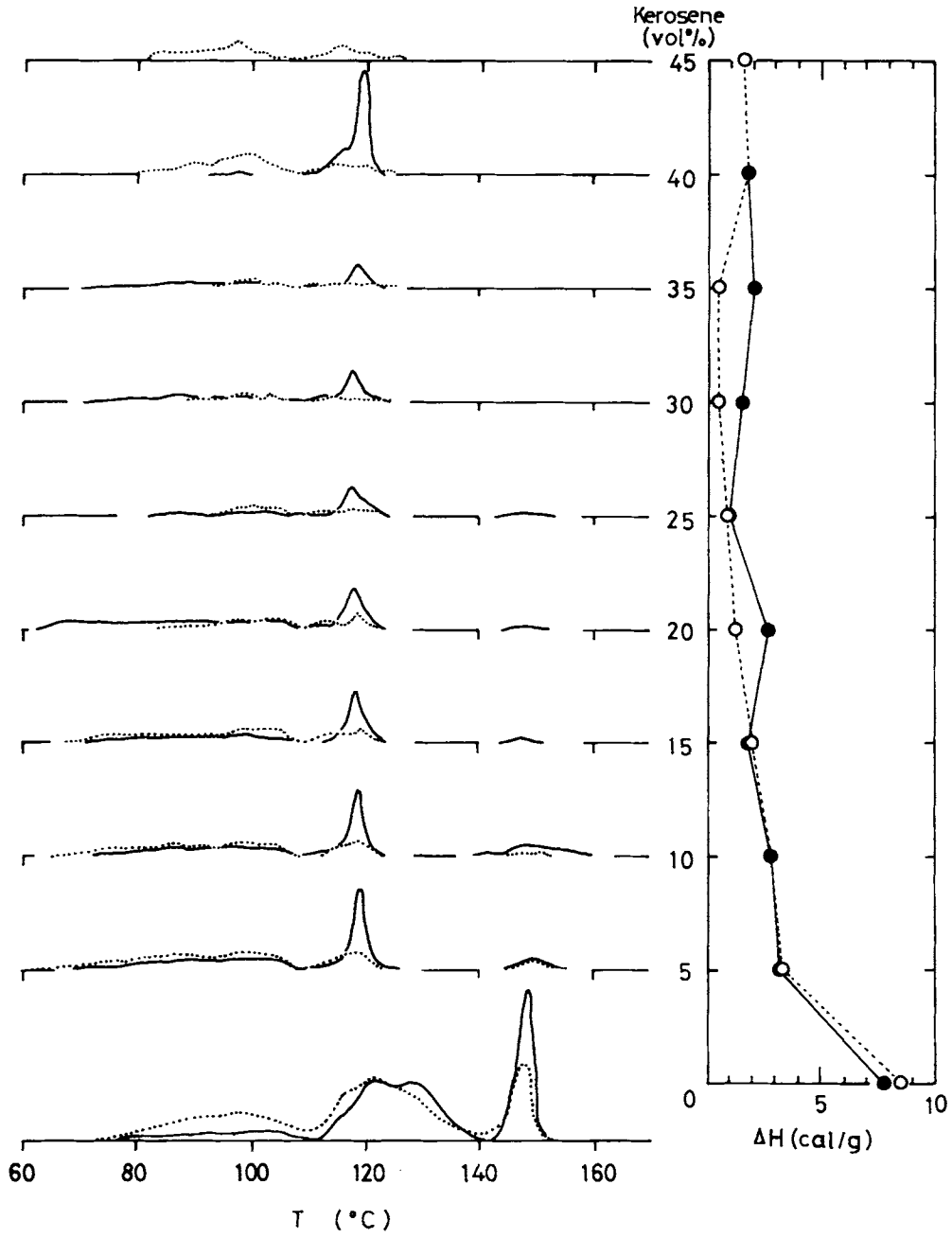

Figure 6 DSC analysis for each fractional polymer. Each DSC curve is normalized in terms of enthalpy of fusion. The enthalpy of fusion for each fraction is plotted at the right side of the figure: (solid lines) A-1; (dashed lines) A-2.

area surrounded by each GPC curve and the base line is normalized with the weight fraction of each fraction, setting the weight of the whole polymer of A-1 or A-2 at one. The fractions F5–F30 were brought together for the measurement. The fractions F40–F100 of A-2 were also brought together likewise. To compare the whole polymers with each other, A-2 shows a decrease in low molecular weight PP with a weight-average molecular weight (M_w) of about 4000 and a remarkable increase in high molecular weight PEP, especially in PEP with a weight-average molecular weight of over 100,000. The F35 fraction was found to be a mixture of more than at least two amorphous PEP components with different

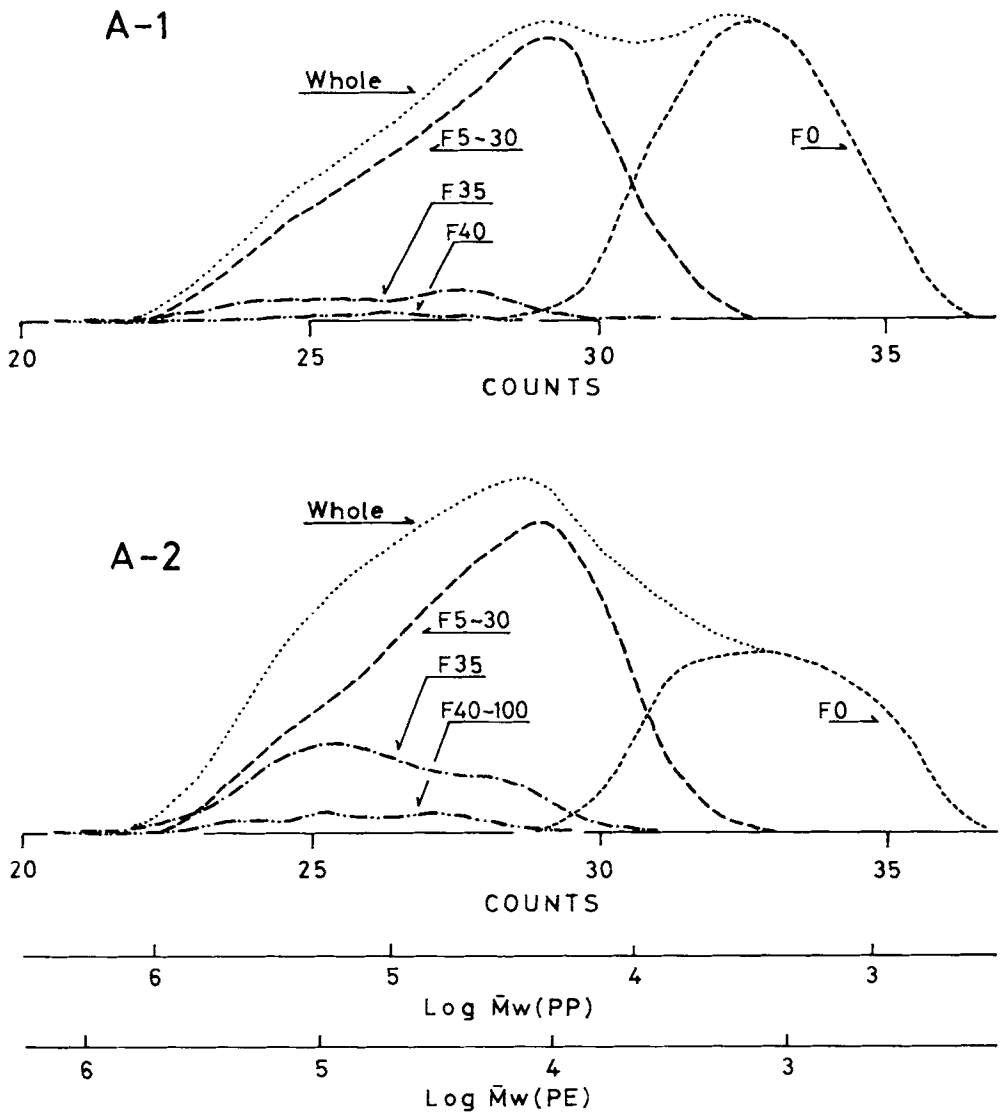

Figure 7 Results of the molecular weight measurement with GPC for fractional polymers of A-1 and A-2.

molecular weights. In addition, the F35 of A-2, as compared with the F35 of A-1, is characteristic in that the shape of the bimodal molecular weight distribution is reversed owing to an increase in the high molecular weight PEP component. This suggests that, in the molding of block PP-A, the annealing treatment makes the high molecular weight amorphous PEP readily extractable with *n*-heptane by changing the morphology.

Phenomena at Interfacial Area by Annealing

The effects of annealing occurring in the solid phase of block PP-A can be postulated from the data described above.

First, PEP diffuses into the PP and PE phases on annealing according to the result in the preceding paper.[6] This diffusion produces layers of interpenetration of molecular segments in the mutually immiscible polymer interfaces of PP/PEP and PEP/PE. These interfacial thicknesses can be thermodynamically calculated; for instance, by use of eq. (1) and the parameters in Table III based on the theory of Helfand and Sapse,[16] the interfacial thickness a_i (1) between the PP phase and the PEP phase of block PP-A as shown in Figure 8 can be calculated to be 70 Å at 25°C:

$$a_i = 2\left(\frac{\beta_A^2 + \beta_B^2}{2\alpha}\right)^{1/2} \quad (1)$$

Table III Physical Parameters of Polymers

Polymer	δ[b] $(cal/cm^3)^{1/2}$	Density (mol/cm^3)	$\langle R^2\rangle^{1/2}/M^{1/2} \times 10^9$[c] $(cm/g^{1/2})$	$b \times 10^8$ (cm)	$\beta \times 10^9$ $(cm^{-1/2})$
PP (amorphous)	7.38	0.0202	7.65	5.0	2.90
PE (amorphous)	8.03	0.0305	9.50	5.0	3.56
PEP[a]	7.59	0.0234	No data	5.0[d]	3.12

[a] Ethylene content is 40 mol %.
[b] Calculated from Hoy's molar attraction constants.
[c] Ref. 18.
[d] Estimated from b values of PP and PE.

α and β_i^2 are represented as follows:

$$\alpha = (1/kT)(\delta_A - \delta_B)^2 \quad (2)$$

$$\beta_i^2 = (1/6)\rho_i b_i^2 \ (i = A \text{ or } B) \quad (3)$$

where δ is the Hildebland solubility parameter; k, the Boltzmann constant; ρ_i, the density of the pure polymer; and b_i, the effective length per monomer unit, chosen so that the mean-square end-to end distance is Zb_i^2. (Z is the degree of polymerization.) Hoy's group molar attraction constants are used to calculate the solubility parameter of PEP, whose ethylene content is 40 mol % equal to that of the important component of PEP in block PP-A. The interfacial thickness estimated by the theory of Meier–Inoue,[17] on the other hand, is 90 Å at 25°C, which is in good agreement with the value by the theory of Helfand and Sapse.[16]

The interfacial thickness a_i (2) between the PEP phase and the PE phase of block PP-A can also be calculated to be 37 Å at 25°C. However, the actual a_i (1) and a_i (2) would be a few angstroms larger than those theoretical values because the composition of PEP near the interface with PP and PE must be a gradient.

However, the diffusion phenomenon in the PP/PEP interface observed by the scanning electron microscope (SEM) is so profound that the domain size of PEP distinctly decreases, and, hence, the interface thickness would be estimated to be several thousand angstroms,[6] which is also supported by the prediction of the thickness of the transitional layer using the difference on the extractability with n-heptane in Table I. Its value corresponds, indeed, to 10 times the theoretical one. Therefore, the thickening of the interfacial layer observed with SEM appears to differ from the formation of the layer of interpenetration as thermodynamically expected. It would be a complex phenomenon induced by the recrystallization, the polymer segregation, and other factors such as the heat convection or the difference of coefficients of thermal expansion.

Accordingly, to avoid confusion in this section, the interpenetration layer of molecular segments as expected from thermodynamics will be called the "segmental interfacial layer" and that between phases as observed via the annealing effect in the

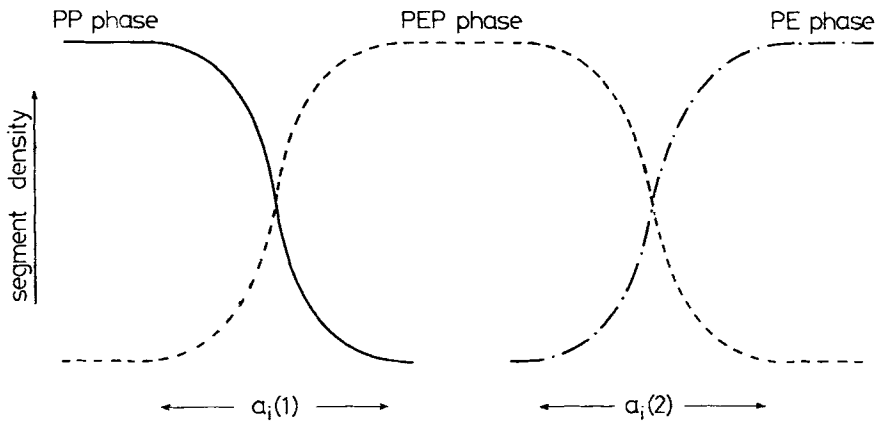

Figure 8 Physical picture of the interfacial region of PP/PEP/PE system in block PP-A. Regions of $a_i(1)$ and $a_i(2)$ show the thickness of the interfacial layers between each phase.

present study will be called the "macroscopic interfacial layer."

Next, as to the recrystallization on annealing, the PP matrix and the PE domain initially undergo recrystallization. Along with this, the diffused, highly isotactic, low molecular weight PP and the diffused PEP with the crystallinity of propylene or ethylene also undergo the recrystallization on PP or PE crystals, so as to be fixed in the crystal region of PP or PE, and so to become difficultly extractable with *n*-heptane. The recrystallization, effecting compatibilization in the interface, is to increase the thickness of the macroscopic interfacial layer and to contribute to the increase in bonding strength in the interfaces PP/PEP and PEP/PE.

Furthermore, as to the components rejected from crystal regions on annealing, atactic PP and amorphous high molecular weight PEP in crystal regions (chiefly in spherulites) migrate into amorphous regions (on spherulite interfaces or in PEP domains) along with their recrystallization. It has been confirmed by an experiment with small-angle neutron scattering that atactic PP and isotactic PP are miscible in a melt state at 200°C but immiscible at room temperature.[19] Amorphous PEP and PP also are entirely immiscible in a melt state. The recrystallization, therefore, has the aspect of a process to promote the rejection of segments incapable of rearrangement in a crystal region. As described hitherto, the phenomenon of segregation of crystalline and amorphous polymers on annealing is an important finding of the present study. The amorphous high molecular weight PEP, migrating into spherulite interfaces and PEP domains as the result of segregation, must further increase the breaking strength at the interface.[1]

CONCLUSIONS

The following complex phenomena in solid phases are the significant causes for the improvement in impact strength (TIS, Tb) on annealing of moldings of block PP consisting of PP/(crystalline PEP + amorphous PEP)/PE.

Crystalline PEP undergoes the recrystallization at the interface with the PP matrix or PE domain, resulting in an increase in miscibility in the interface and a thickening of the segmental interface layer. It effects thereby an increase in the bonding strength and an improvement in the breaking strength in the interfaces of PP/PEP and of PEP/PE.

The recrystallization of the PP matrix is followed by migration of atactic PP and high molecular weight amorphous PEP from the crystalline region to the amorphous region (spherulite interface or PEP domain). As the result, the glass transition temperature of the system as a whole is lowered, the interfacial bonding strength increases, and, hence, the interfacial strength against impact stress is improved.

When block PP is annealed, ultimately, the macroscopic interfacial layers of PP/PEP and PEP/PE are thickened to become 10 times the theoretical thickness by way of not only the recrystallization and the polymer segregation but also the polymer diffusion given rise to by some cause such as the heat convection or the difference in coefficients of thermal expansion, so as to effect an increase in the bonding strength and breaking strength at the PP/PEP and PEP/PE interfaces.

The authors would like to thank Mr. Yoshito Eda for his assistance of the ^{13}C-NMR measurement of all the polymer samples.

REFERENCES

1. T. Kuroda, *Kobunshi,* **28,** 714 (1979).
2. M. Kojima, *Zairyo-kagaku,* **18,** 233 (1982).
3. T. Takahashi, H. Mizuno, and E. L. Thomas, *J. Macromol. Sci. Phys.,* **B22,** 425 (1983).
4. J. Karger-Kocsis, K. Kiss, and V. N. Kuleznev, *Polym. Commun.,* **25,** 122 (1984).
5. M. Ishikawa and I. Narisawa, *Polym. Prepr. Jpn.,* **33,** 2379 (1984).
6. J. Ito, K. Mitani, and Y. Mizutani, *J. Appl. Polym. Sci.,* **00,** 00 (1992).
7. L. C. E. Struik, *Polymer,* **28,** 1521 (1987).
8. L. C. E. Struik, *Polymer,* **28,** 1534 (1987).
9. J. Ito, K. Mitani, and Y. Mizutani, *J. Appl. Polym. Sci.,* **29,** 75 (1984).
10. V. Desreux, *Rec. Trav. Chim. Pays-Bas.,* **68,** 789 (1949).
11. R. W. Hall, *Techniques of Polymer Characterization,* P. W. Allen, ed., Butterworths, London, 1959, p. 113.
12. A. Saijo, S. Hayashi, F. Hamada, and A. Nakajima, *Kobunshi-kagaku,* **24,** 775 (1967).
13. T. Ogawa, Y. Suzuki, S. Tanaka, and S. Hoshino, *Kobunshi-kagaku,* **27,** 356 (1970).
14. J. Ito, K. Mitani, and Y. Mizutani, *J. Appl. Polym. Sci.,* **30,** 497 (1985).
15. J. Boor, *Ziegler-Natta Catalysts and Polymerization,* Academic Press, New York, 1979, Chap. 20.
16. E. Helfand and A. M. Sapse, *J. Chem. Phys.,* **62,** 1327 (1975).
17. D. J. Meier and T. Inoue, *Polym. Prepr. Jpn.,* **24,** 293 (1975).
18. J. Brandrup and E. H. Immergut, Eds., *Polymer Handbook,* 3rd ed. Wiley, New York, 1989, Chap. VII.
19. D. J. Lohse, *Polym. Eng. Sci.,* **26,** 1500 (1986).

Received October 14, 1991
Accepted January 23, 1992